PIBB 生物化学与生物物理进展
Progress in Biochemistry and Biophysics
2010, 37(12): 1313~1322
www.pibb.ac.cn

高内涵法探讨土槿皮乙酸对 MCF-7 细胞抑制作用的机制 *

段绍维 徐 波 陈云利 李 敏 傅宏征 ** 崔景荣 **
(北京大学天然药物及仿生药物国家重点实验室，北京 100191)

摘要 土槿皮乙酸(pseudolaric acid B，PAB)是土槿皮(金钱松根皮)的主要生物活性成分，对多种人肿瘤细胞有细胞毒性作用．高内涵分析(high content analysis，HCA)是一种基于荧光显微技术的新技术，它以细胞为研究对象，可以同时对多个荧光靶点的荧光强度、分布，以及细胞形态进行自动化定量分析．利用高内涵分析、流式细胞术研究 PAB 对人乳腺癌 MCF-7 细胞抑制作用的机制．磺酰罗丹明实验显示，PAB 抑制 MCF-7 细胞增殖，且呈现出剂量和时间依赖性，72 h IC_{50} 为 (1.80±0.33) μmol/L．流式细胞术碘化丙锭(PI)单染显示 PAB 作用 24 h，可致 MCF-7 细胞 G2/M 期比例增至 93% 以上，annexin V-FITC 和 PI 双染显示 PAB 促进 MCF-7 细胞凋亡．高内涵分析显示：PAB 作用 16 h，MCF-7 细胞有丝分裂指数可达 40% 左右，伴有 cyclin B1 含量增加；PAB 促进微管解聚，干扰有丝分裂二极纺锤体形成；PAB 引起线粒体增生；PAB 导致“葡萄串样”细胞核形成，提示有丝分裂滑脱．结果表明，PAB 抑制 MCF-7 细胞增殖、促进 MCF-7 细胞凋亡，这些作用可能与其促进微管蛋白解聚、干扰二极纺锤体形成、阻滞有丝分裂、促进线粒体增生有关．

关键词 高内涵分析，土槿皮乙酸，MCF-7 细胞，微管，有丝分裂阻滞，凋亡
学科分类号 R961，R965.1，R979.1
DOI: 10.3724/SP.J.1206.2010.00335

土槿皮为松科植物金钱松(*Pseudolarix kaempferi* Gordon)的根皮，是一种治疗皮肤真菌感染的传统中药．从土槿皮中分离得到的二萜类化合物土槿皮乙酸(pseudolaric acid B，PAB；图 1)，是土槿皮抗真菌的主要成分[1]．体外实验显示，PAB 对多种人肿瘤细胞系的增殖有抑制作用[2]，而且相对于人正常细胞表现出选择性(PAB 作用于肿瘤细胞的 IC_{50} 约为正常细胞的 1/100)[3-4]，诱导人白血病、胃癌、肝癌、结肠癌、乳腺癌、宫颈癌和黑色素瘤等恶性肿瘤细胞凋亡[3, 5-10]，抑制血管生成[11-12]，促进微管解聚[4, 11]．高内涵分析(high content analysis)是一种基于荧光显微技术的自动化技术，它以结构完整的细胞作为研究对象，可以同时对多个荧光靶点的荧光强度、分布，以及细胞形态进行自动化的定量分析，可用于药物机制研究或者大规模药物筛选[13-14]．乳腺癌是妇女最多发的恶性肿瘤，而且其发病率呈逐渐上升趋势．本文利用高内涵分析等技术研究 PAB 对人乳腺癌 MCF-7 细胞抑制作用的机制．

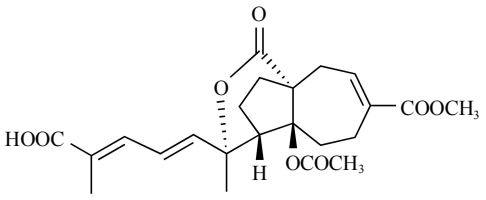

Fig. 1 Chemical structure of pseudolaric acid B (PAB)

1 材料与方法

1.1 试剂和药品

RPMI-1640 细胞培养基购自 Gibco 公司；胎牛

* 国家“十一五”攻关项目, 重大新药创制资助项目(2009ZX09301-010).
** 通讯联系人.
崔景荣. Tel: 010-82802467, E-mail: jrcui@bjmu.edu.cn
傅宏征. Tel: 010-82805212, E-mail: drhzfu@yahoo.com.cn
收稿日期：2010-06-25，接受日期：2010-09-30

血清购自杭州四季青生物工程材料有限公司；磺酰罗丹明 B(sulforhodamine B，SRB)、核糖核酸酶 A (RNase A)、碘化丙锭(propidium iodide，PI)购自 Sigma-Aldrich 公司；annexin Ⅴ凋亡检测试剂盒由北京大学人类疾病基因研究中心提供．高内涵分析试剂盒 Mitotic Index Kit (K0500011)、Cyclin B1 Activation Kit(8404402)、Cytoskeletal Rearrangement Kit(8402402)、Multiparameter Cytotoxicity 2 Multiplex Kit(8400002)购自 Cellomics 公司(Pittsburgh，PA，USA)．兔抗 pHH3 IgG、Alex Fluor 488 羊抗兔 IgG 取自 Mitotic Index Kit(K0500011)；鼠抗 cyclin B1 抗体、DyLight™ 549 羊抗鼠 IgG、DAPI 取自 Cyclin B1 Activation Kit(8404402)；DY554- 鬼笔环肽、鼠抗微管蛋白抗体、DyLight™ 649 羊抗鼠 IgG 取自 Cytoskeletal Rearrangement Kit(8402402)；线粒体染液取自 Multiparameter Cytotoxicity 2 Multiplex Kit(8400002)．高内涵分析使用的打孔液、封闭液取自前述各试剂盒．

PAB 由北京大学天然药物及仿生药物国家重点实验室傅宏征教授制备，溶于 DMSO，储存于 –20℃，储备液用 RPMI-1640 完全培养基稀释为不同浓度．作用于细胞时 PAB 终溶液的 DMSO 含量为 0.5%(体积比)．紫杉醇注射液购自海口市制药厂；长春碱取自 Mitotic Index Kits(K0500011)．

1.2 细胞培养

人乳腺癌细胞 MCF-7 由本室保存，以含有 10% 灭活胎牛血清、100 U/ml 青霉素、100 mg/L 链霉素的 RPMI-1640 培养基于 37℃、5% CO_2、饱和湿度培养箱中培养．

1.3 磺酰罗丹明实验

取对数生长期 MCF-7 细胞 5000 个 / 孔接种于 96 孔板(Costar 3599)．培养箱中培养 24 h 后吸去培养基，加入不同浓度 PAB 溶液 200 μl/ 孔．含 0.5% DMSO 的 RPMI-1640 完全培养基和 1 μmol/L 紫杉醇分别作为阴性和阳性对照．每种处理方式设 6 个平行孔．加药后 0、48、72 h，参考 Skehan 的方法[15]，在培养基液面上加 50 μl 50% 三氯乙酸(trichloroacetic acid，TCA)，4℃ 固定 1 h，自来水冲洗，0.4% SRB 染色，1% 乙酸冲洗，10 mmol/L Tris 溶解细胞结合的 SRB．最后用酶联免疫检测仪在 540 nm 波长测定吸光度(*A*)值，计算抑制率、IC_{50} 和 GI_{50}[16]．抑制率=$(C-T)/C\times100\%$，IC_{50} 为抑制率等于 50% 时的药物浓度，GI_{50} 为 $(T-T0)/(C-T0)$= 50% 时的药物浓度．*T*、*C*、*T*0 分别为药物作用后的 *A* 值、阴性对照的 *A* 值、药物作用 0 h 的 *A* 值．

1.4 流式细胞术

取对数生长期 MCF-7 细胞 1×10^5 个 /ml 接种于培养瓶．24 h 后加入不同浓度 PAB 溶液，含 0.5% DMSO 的 RPMI-1640 完全培养基和 2.5 μmol/L 紫杉醇溶液(终浓度)分别作为阴性和阳性对照．

1.4.1 细胞周期(PI 单染)．收集细胞，经 PBS 洗涤后取约 1×10^6 个细胞，70% 冷乙醇固定过夜．固定后的细胞经 PBS 洗涤，RNase A(终浓度 100 mg/L) 37℃ 孵育 30 min，再次 PBS 洗涤，筛网过滤，PI 染色(PI 终浓度 50 mg/L)，上流式细胞仪用 CellQuest 软件分析细胞周期．

1.4.2 细胞凋亡(annexin V-FITC+PI)．用 annexin Ⅴ凋亡检测试剂盒处理细胞．收集细胞，经 PBS 洗涤后取约 1×10^6 个细胞，在结合缓冲液中用 annexin Ⅴ-FITC 室温孵育 15 min，筛网过滤，加入 PI，上流式细胞仪用 CellQuest 软件分析凋亡细胞比例．

1.5 高内涵分析(high content analysis，HCA)

取对数生长期 MCF-7 细胞，稀释细胞悬液至适宜密度(多参数细胞周期分析、细胞核和线粒体分析 5×10^4 个 /ml，微管和微丝分析 3×10^4 个 /ml)，每孔 100 μl 加入 96 孔板(Costar 3599)，96 孔板事先用 0.1% 明胶包被．24 h 后加入不同浓度 PAB 溶液 50 μl/ 孔，含 0.5% DMSO 的 RPMI-1640 完全培养基为阴性对照，1 μmol/L 紫杉醇(终浓度)、1 μmol/L 长春碱(终浓度)为阳性对照．

1.5.1 多参数细胞周期分析．加药后 24 h，加入 37℃ 预热的 16% 甲醛溶液 50 μl/ 孔(终浓度 4%)室温固定 30 min，再用打孔液、封闭液分别作用 15 min．鼠抗 cyclin B1(1∶500)、兔抗磷酸化组蛋白 H3(phospho-histone H3, pHH3, 1∶400)50 μl/ 孔室温孵育 1 h．PBS 洗 2 次．细胞核染料 DAPI (1∶2000)、DyLight™ 549 羊抗鼠 IgG(1∶500)、Alex Fluor 488 羊抗兔 IgG(1∶250) 50 μl/ 孔室温避光孵育 30 min．PBS 洗 2 次．使用高内涵分析设备 KineticScan Reader(Cellomics, Pittsburgh, PA, USA) 采集荧光图像，配套软件 Cell Cycle BioApplication 计算 cyclin B1 荧光强度和有丝分裂指数(mitotic index，*MI*)．因为 pHH3 阳性可视为 M 期细胞的标志[17]，因此 *MI* = 100% × M 期细胞数 / 总细胞数= 100% × pHH3 阳性细胞数 /DAPI 着色细胞数．

1.5.2 微管和微丝．加药后 8 h，MCF-7 细胞经固定、打孔、封闭(同 **1.5.1**)，室温下用鼠抗微管蛋

白抗体(1∶1 000)孵育 1 h，PBS 洗 2 次，DAPI (1∶2 000)和 DyLight™ 649 羊抗鼠 IgG(1∶1 000)室温避光孵育 30 min，PBS 洗 2 次．Compartmental Analysis BioApplication 计算微管蛋白荧光强度．

1.5.3　细胞核和线粒体．加药后 23.5、47.5 h，加入线粒体染液 60 μl/ 孔作用 30 min，加入 37℃ 预热的 16% 甲醛 70 μl/ 孔(终浓度 4%)室温固定 30 min，PBS 洗 1 次，DAPI(1∶2 000) 50 μl/ 孔室温避光孵育 30 min，PBS 洗 2 次．Compartmental Analysis BioApplication 分析细胞核形态和线粒体荧光强度．

1.6　统计学分析

计量资料用 $\bar{x} \pm s$ 表示，加药组和阴性对照之间的比较分析采用 Student's t 检验．

2　实验结果

2.1　PAB 对细胞增殖的抑制作用

PAB 作用 MCF-7 细胞 24 h 后，倒置显微镜下见大量细胞变圆，作用 48 h 或 72 h 后，见细胞数目少于阴性对照孔，细胞碎片增多，可见体积变大的细胞．SRB 实验结果显示，PAB 对 MCF-7 细胞增殖的抑制作用表现出剂量和时间依赖性(图 2)．PAB 作用 72 h 的 IC_{50} 为(1.80±0.33) μmol/L．PAB 作用 48 h 和 72 h 的 GI_{50} 分别为(1.85±0.30) μmol/L 和(1.43±0.26) μmol/L．

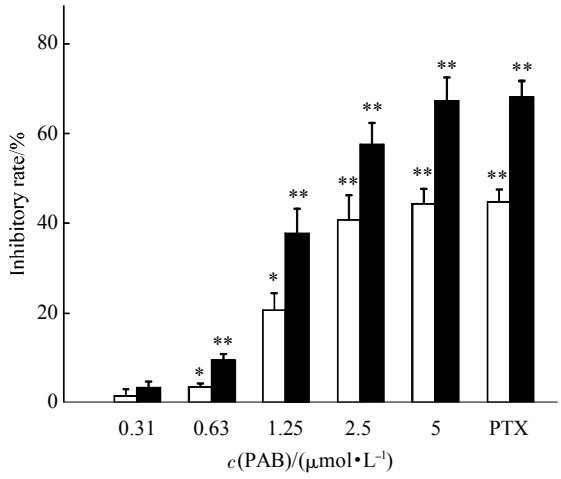

Fig. 2　Effect of PAB on the proliferation of MCF-7 cells

MCF-7 cells were exposed to increasing concentrations of PAB for 48 h or 72 h, and 1 μmol/L paclitaxel (PTX) was used as positive control. Inhibition rates were determined by SRB assay. Each data point represents the $\bar{x} \pm s$ deviation of 3 independent experiments. $^*P < 0.05$, $^{**}P < 0.01$, *vs* solvent control. □: 48 h; ■: 72 h.

2.2　PAB 导致细胞 G2/M 期阻滞、有丝分裂指数升高、cyclin B1 含量升高

2.2.1　PAB 导致 G2/M 期阻滞．不同浓度 PAB 作用于 MCF-7 细胞 24 h，PI 染色后流式细胞术分析细胞周期．结果显示随着 PAB 浓度升高(0～1.25 μmol/L)，S 期细胞比例逐渐增大．PAB 浓度≥2.5 μmol/L 时，S 期细胞比例减小，G2/M 期比例明显增大, 达 93% 以上(图 3a). 2.5 μmol/L PAB 作用于 MCF-7 细胞 12、24 h，G2/M 期细胞比例增大，表现出时间依赖性(图 3b)．高内涵法通过 DAPI 荧光强度分析细胞周期，5 μmol/L PAB、1 μmol/L 紫杉醇作用于 MCF-7 细胞 16 h 后，细胞 4 N 峰升高(图 4a)，与流式细胞术结果类似．

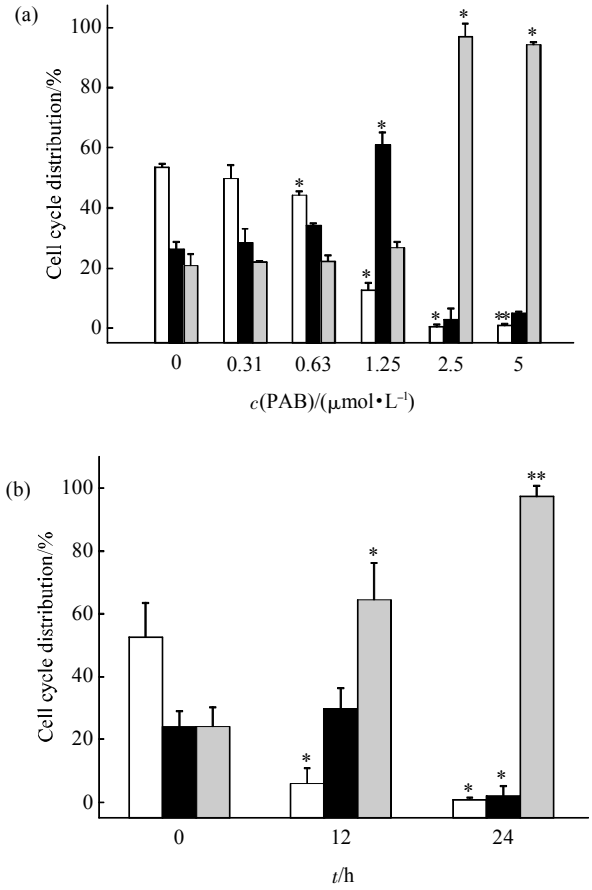

Fig. 3　Effect of PAB on cell cycle distribution of MCF-7 cells

MCF-7 cells were stained with PI, and cell cycle distribution was determined by flow cytometry analysis of DNA content. (a) MCF-7 cells were exposed to increasing concentrations of PAB for 24 h. Data were given as $\bar{x} \pm s$, n=2. (b) MCF-7 cells were exposed to 2.5 μmol/L PAB for 12 h or 24 h. Data were given as $\bar{x} \pm s$, n=3. $^*P < 0.05$, $^{**}P < 0.01$, *vs* solvent control. □: G0/G1; ■: S; ▨: G2/M.

2.2.2　PAB 导致 *MI* 升高．0.5% DMSO、不同浓度的 PAB 或 1 μmol/L 紫杉醇作用于 MCF-7 细胞 16 h.

PAB 作用后高表达 pHH3、cyclin B1 的细胞增多，高表达 pHH3 者可见染色质凝集(图 4a). 定量分析见 PAB 导致 *MI* 升高，且表现出剂量依赖性(图 4b). PAB 导致细胞 cyclin B1 含量增高，且表现出剂量依赖性(图 4c). 另外，从图 4a 可见 pHH3 阳性细胞常伴随着较亮的 cyclin B1 荧光. 为了比较 M 期细胞(pHH3 阳性)和间期细胞(pHH3 阴性)的 cyclin B1 含量，选择适宜的 pHH3 荧光强度作为临界值，根据此临界值区分 M 期细胞和间期细胞，计算其各自的 cyclin B1 荧光强度. 结果显示，在溶剂对照组、PAB 组、紫杉醇组中，M 期细胞 cyclin B1 含量都要高于间期细胞(图 4d).

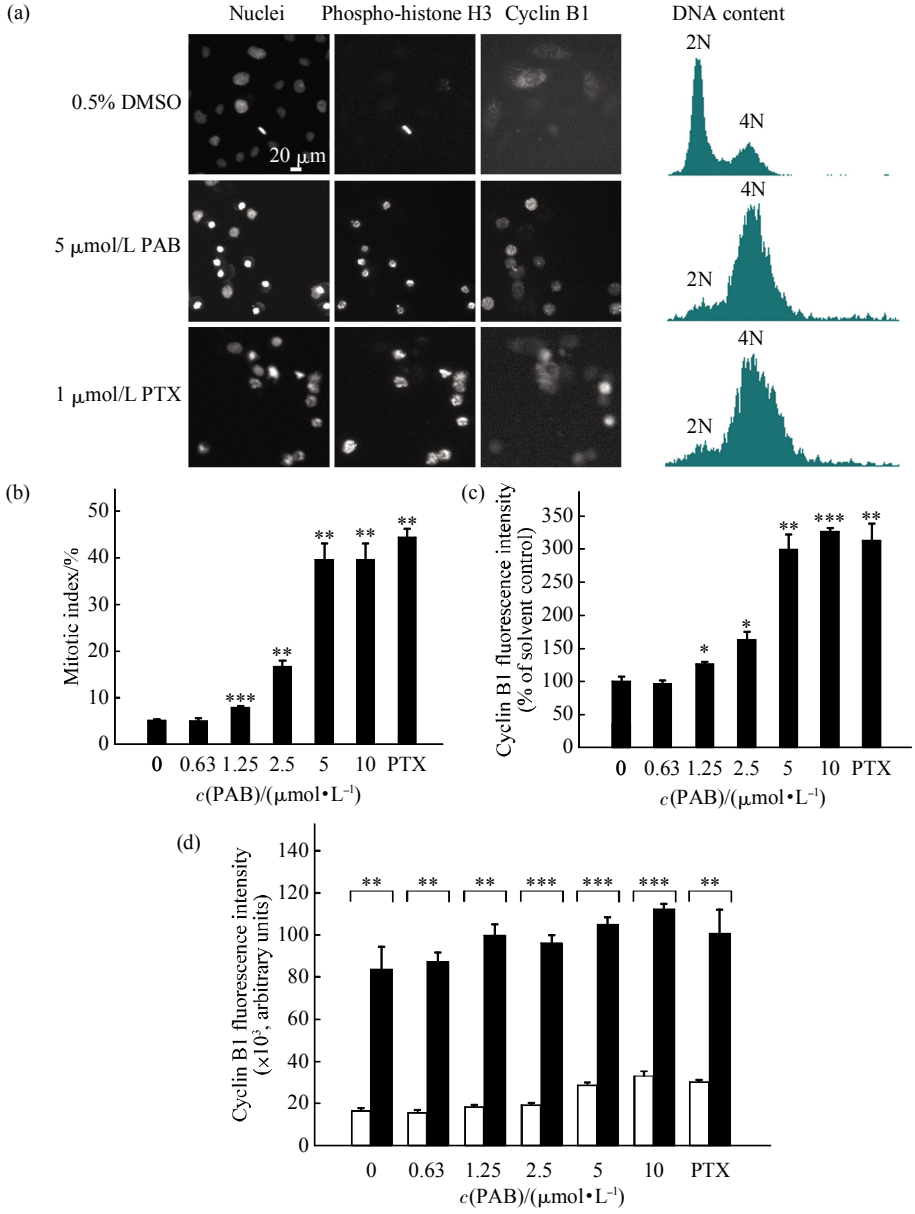

Fig. 4　Multiparametric analysis of cell cycle by high content analysis

MCF-7 cells were treated for 16 h with 0.5% (*v*/*v*) DMSO, indicated concentrations of PAB or 1 μmol/L paclitaxel (PTX). (a) Representative images of MCF-7 cells treated with 0.5% DMSO, 5 μmol/L PAB or 1 μmol/L paclitaxel. Cells were simultaneously stained for nucleus, phospho-histone H3 and cyclin B1. PAB and paclitaxel induced increases of phospho-histone H3-positive cells (mitotic cells) and cyclin B1- highly expressed cells. Right panels represent DNA content distribution obtained from DAPI staining. Images were captured with KineticScan Reader (Cellomics, Pittsburgh, PA, USA) with a 10× objective. The background of some images of the same fluorescence target appears different because images were displayed in contrast stretched mode to emphasize weak fluorescence, while quantitative data were not stretched. (b) Quantitation of mitotic index of MCF-7 cells. PAB induced an increase in mitotic index in a dose-dependent manner. (c) PAB induced an increase in cyclin B1 fluorescence intensity in a dose-dependent manner. (d) Cyclin B1 fluorescence intensity of mitotic cells was compared with that of interphase cells for each treatment. Mitotic cells showed higher cyclin B1 fluorescence intensity than interphase cells. Quantitation in (b), (c) and (d) was performed with the Cell Cycle BioApplication (Cellomics, Pittsburgh, PA, USA), and at least 600 cells per well were analyzed. Data were given as $\bar{x} \pm s$, n=3. **P* < 0.05, ***P* < 0.01, ****P* < 0.001, *vs* solvent control. □ in (d): Interphase cells; ■ in (d): Mitotic cells.

2.3　PAB 干扰两极纺锤体形成

高内涵分析采集的荧光图片显示，溶剂对照孔可见正常的有丝分裂中期细胞(图 5)，染色体排列成赤道板(equatorial plate)，微管形成两极纺锤体．2.5、5 μmol/L PAB 作用于 MCF-7 细胞后 8 h，M 期细胞染色体凝集但是分布紊乱，未见赤道板，微管染色淡，未见两极纺锤体形态．荧光图片中(2.5、5、10 μmol/L PAB 共 90 个视野约 1 500 个细胞)未发现一个正常的有丝分裂中期细胞．1 μmol/L 紫杉醇作用 8 h 后也未能见到两极纺锤体.

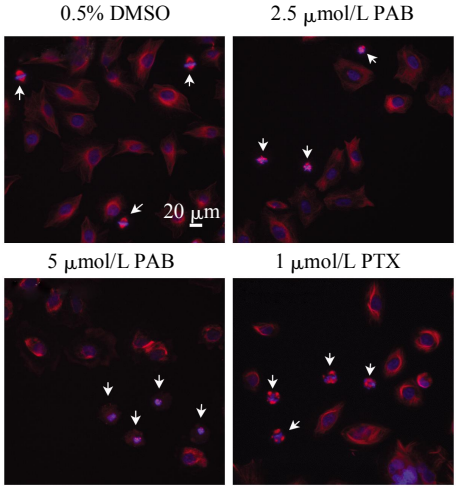

Fig. 5　PAB and paclitaxel induced spindle abnormalities in MCF-7 cells

MCF-7 cells were treated for 8 h with 0.5% (*v*/*v*) DMSO, indicated concentrations of PAB or 1 μmol/L paclitaxel. Cells were then counterstained for nucleus (blue) and tubulin (red). Representative images of mitotic cells were shown (arrows). Metaphase cells in control wells have normal bipolar spindles, and their chromosomes congregate to the equator forming the equatorial plate (left upper panel). Both PAB and paclitaxel arrested cells in prometaphase and induced spindle abnormalities. Images were captured with KineticScan Reader (Cellomics, Pittsburgh, PA, USA) with a 20 × objective. Images were displayed in contrast stretched mode to emphasize weak fluorescence.

2.4　PAB 促进间期细胞微管解聚

PAB 作用于 MCF-7 细胞 8 h，纤维状肌动蛋白(F-actin)和微管蛋白(tubulin)行免疫荧光染色后作高内涵分析．从图 6a 可见 2.5 μmol/L PAB 作用后细胞微管纤维连续性较溶剂对照差，出现更多中断，5 μmol/L PAB 作用后微管蛋白荧光强度明显减弱，细胞淡染，核周残余较亮的荧光团块．1 μmol/L 长春碱作用后细胞淡染、核周较亮，但是荧光分布较 PAB 作用后均匀．1 μmol/L 紫杉醇作用后微管蛋白荧光强度明显增强，在核周形成高亮的微管束．定量分析表明(图 6b) 5、10 μmol/L PAB 导致细胞微管蛋白荧光强度减弱，紫杉醇与长春碱分别导致微管蛋白荧光强度增强和减弱．

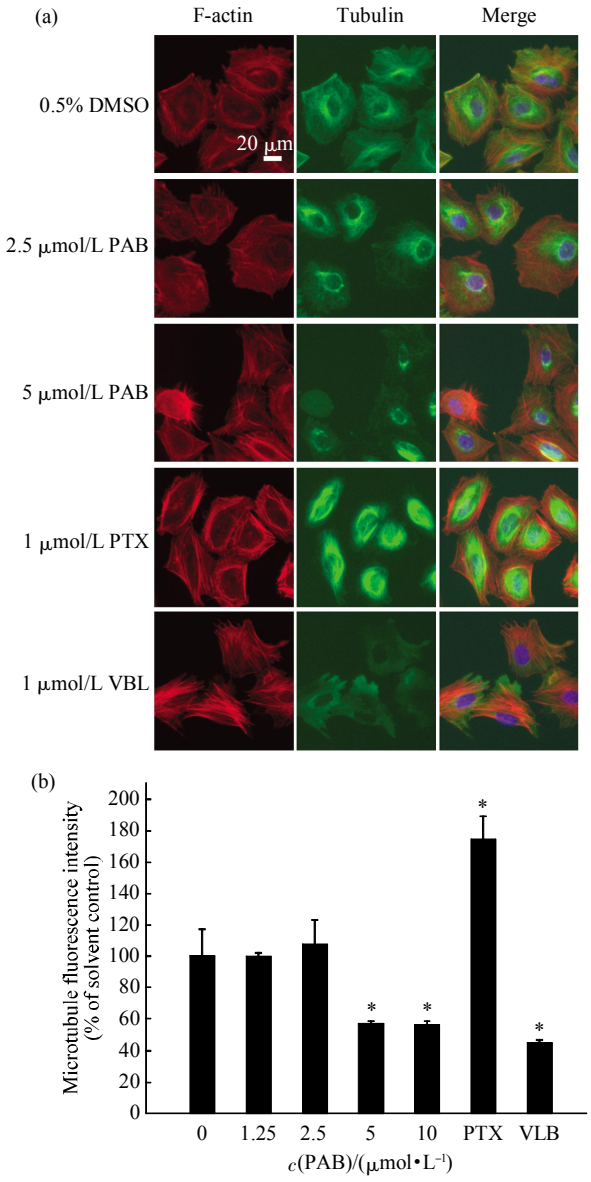

Fig. 6　Effect of PAB, paclitaxel and vinblastine on interphase microtubule networks in MCF-7 cells

MCF-7 cells treated for 8 h with 0.5% (*v*/*v*) DMSO, PAB, paclitaxel (PTX) or vinblastine (VLB) were stained for nucleus (blue), F-actin (red) and tubulin (green). (a) Compared with solvent control, microtubules in cells were slightly disrupted after treatment with 2.5 μmol/L PAB and more completely with 5 μmol/L PAB or 1 μmol/L vinblasinte. On the other hand, cells treated with 1 μmol/L paclitaxel have stabilized microtubule bundles around the nuclei. Images were captured with KineticScan Reader (Cellomics, Pittsburgh, PA, USA) with a 20 × objective. (b) Microtubule fluorescence intensity was quantified using Compartmental Analysis BioApplication (Cellomics, Pittsburgh, PA, USA), and at least 120 cells per well were analyzed. Data were given as $\bar{x} \pm s$, n=3. * P < 0.05, *vs* solvent control.

2.5　PAB 引起细胞核形态改变、线粒体增生

PAB 作用后，MCF-7 细胞形成“葡萄串”样细胞核．1 μmol/L 紫杉醇也引起类似改变(图 7a)．定量分析见 PAB 作用 24、48 h 后，细胞核增大、形状变得不规则，尤以 PAB 浓度≥2.5 μmol/L 时明显(图 7b、7c)．PAB 还导致线粒体荧光强度明显增强，提示线粒体增生．

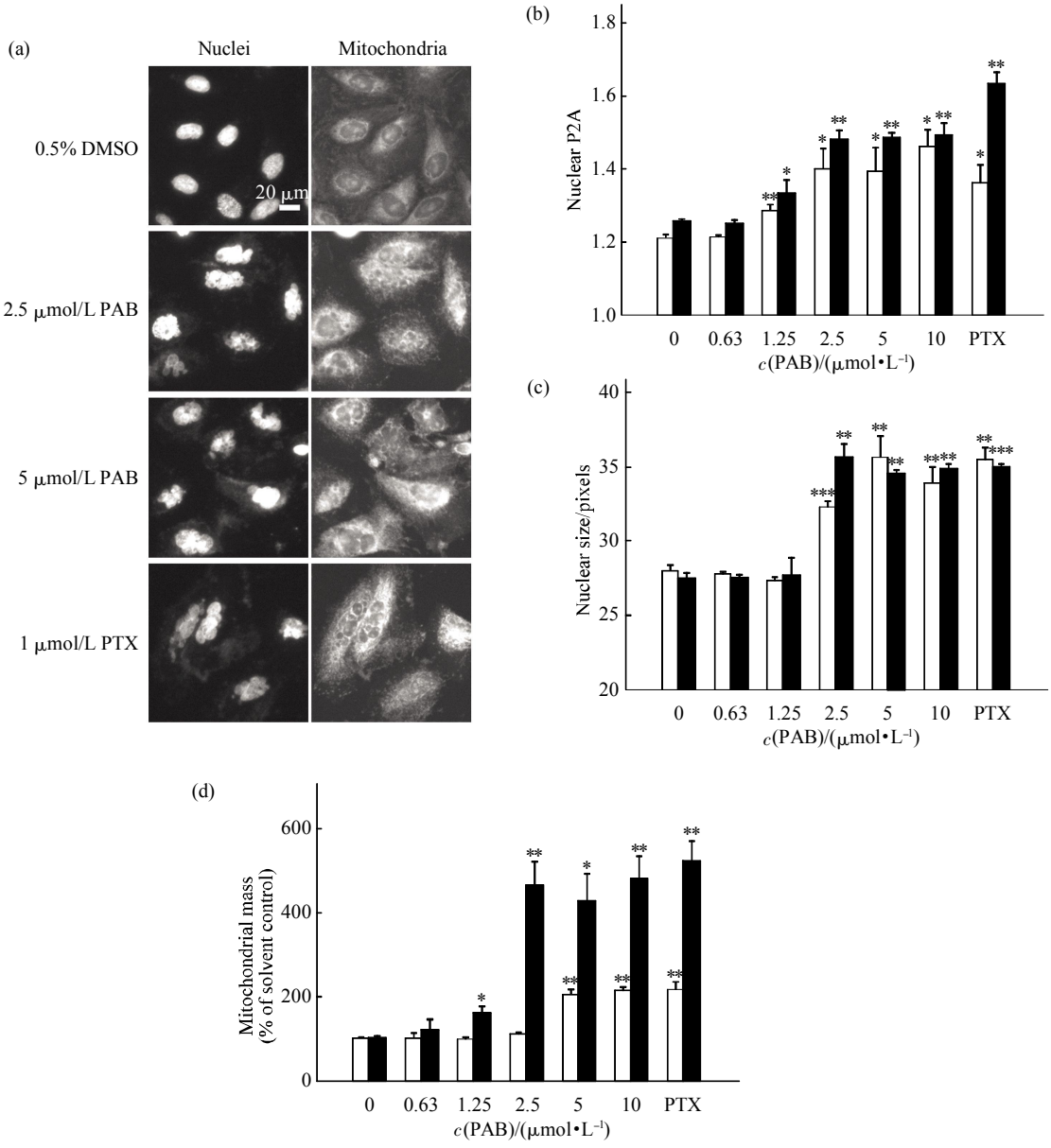

Fig. 7　PAB and paclitaxel induced nuclear morphology and mitochondrial changes in MCF-7 cells

(a) Representative images of MCF-7 cells treated for 48 h with 0.5% (*v*/*v*) DMSO, PAB or paclitaxel (PTX) were stained for nucleus and mitochondrion. PAB (≥2.5 μmol/L) and 1 μmol/L paclitaxel induced giant and grape-like nuclei and increase of mitochondrial fluorescence intensity. Images were captured with KineticScan Reader (Cellomics, Pittsburgh, PA, USA) with a 20× objective. (b) and (c) Quantitation of nuclear size and roundness (P2A). Nuclear size increased while roundness decreased after treatment for 24 h or 48 h with PAB (≥2.5 μmol/L). Nuclear P2A = (perimeter)^2 ÷ (4π × area of nucleus). P2A value is 1 for circle, and irregularly shaped objects have values greater than 1. (d) PAB and paclitaxel induced increase of mitochondrial fluorescence intensity. Quantitation in (b), (c) and (d) was performed with the Compartmental Analysis BioApplication (Cellomics, Pittsburgh, PA, USA), and at least 100 cells per well were analyzed (mitotic cellss were excluded when nuclear size and roundness were measured). Data were given as $\bar{x} \pm s$, n=3. *P < 0.05, **P < 0.01, ***P < 0.001, *vs* solvent control. □: 24 h; ■: 48 h.

2.6　PAB 促进细胞凋亡

不同浓度 PAB 作用于 MCF-7 细胞一定时间，用 annexin V-FITC 和 PI 染色，流式细胞术分析凋亡细胞比例．结果显示，PAB 作用后 72 h, annexin

V-FITC 阳性细胞(早期凋亡细胞 + 晚期凋亡和坏死细胞)比例高于溶剂对照，且表现出剂量依赖性(2.5～10 μmol/L)(图 8a). PAB 5 μmol/L 作用后，annexin V-FITC 阳性细胞比例升高，且表现出时间依赖性(图 8b).

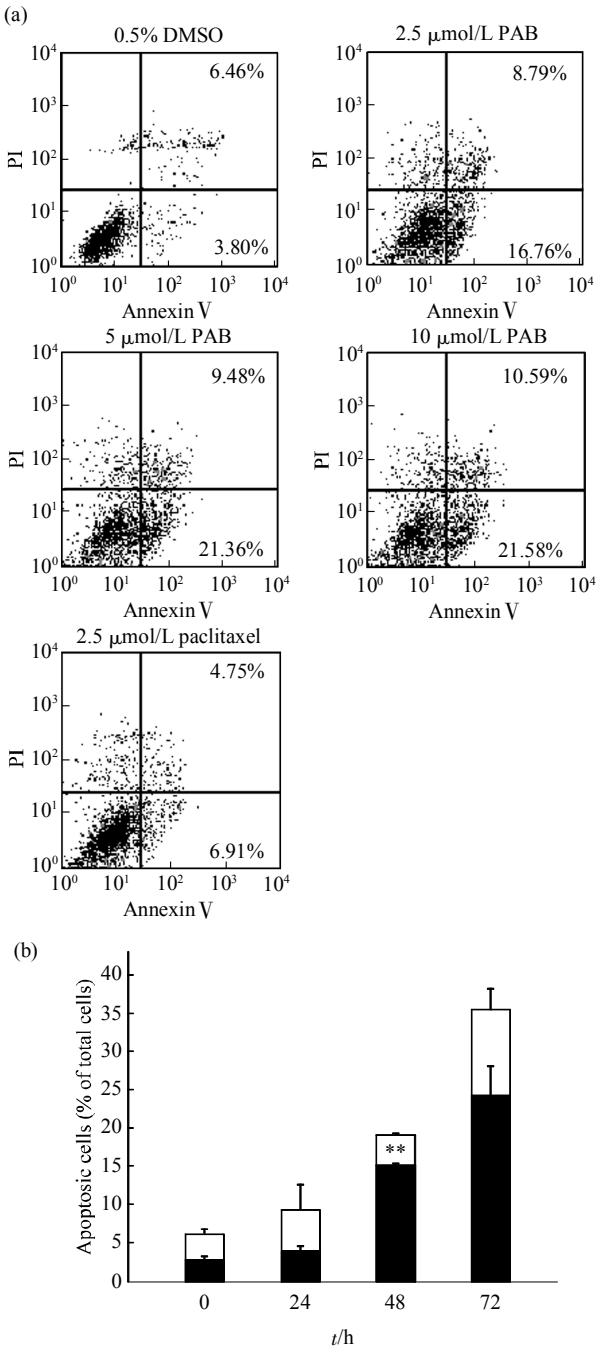

Fig. 8　PAB induced MCF-7 cells apoptosis

MCF-7 cells were stained with annexin Ⅴ-FITC and PI, and percent of apoptotic cells were determined by flow cytometry. (a) MCF-7 cells were exposed to increasing concentrations of PAB for 72 h. (b) MCF-7 cells were exposed to 5 μmol/L PAB for 0 h, 24 h, 48 h and 72 h. Data were given as $\bar{x} \pm s$, n=2. $^{**}P < 0.01$, *vs* solvent control. ■: Early apoptotic cells; □: Late apoptotic or necrotic cells.

3　讨　　论

实验结果显示，PAB 抑制 MCF-7 细胞增殖，使细胞有丝分裂指数增高、cyclin B1 含量增加，干扰有丝分裂期两极纺锤体形成，促进细胞凋亡. 由此可见，PAB 对 MCF-7 细胞的抑制作用可来自两个方面，一是增殖抑制作用，二是包括凋亡在内的细胞毒性作用.

从流式细胞术 PI 单染的实验结果可见，PAB 将 MCF-7 细胞阻滞在 G2/M 期. 高内涵法通过 DAPI 染色也可得到与流式细胞术类似的结果. 不过，PI 或者 DAPI 单染只是通过 DNA 含量对细胞进行分期，不能区分 G2 期和 M 期细胞. 高内涵法直接量化有丝分裂指数，结果显示 PAB 导致有丝分裂指数明显增高. 由此推测 PAB 对 MCF-7 细胞的周期阻滞主要是在 M 期，而非通过激活 G2 期周期检验点把细胞阻滞在 G2/M 期转换处. 有文献报道 PAB 作用于 HepG2 细胞后 G2 期检验点相关蛋白的表达并无明显变化[18]，这与直接测量有丝分裂指数的结果是一致的. 另外流式细胞术显示，浓度≤1.25 μmol/L 的 PAB 作用 MCF-7 细胞 24 h，或者 2.5 μmol/L PAB 作用 12 h 后，S 期细胞比例较阴性对照增加. 考虑出现该现象的原因是，G1 期细胞不断进入 S 期，而有丝分裂阻滞导致新形成的 G1 期细胞减少，所以 S 期比例相应增大. 当然，不排除 PAB 可能导致暂时的 S 期阻滞. DNA 拓扑异构酶Ⅰ抑制是 S 期阻滞的常见原因[19]，不过有文献报道 PAB 对 HL-60 细胞的拓扑异构酶Ⅰ没有抑制作用[3].

细胞有丝分裂受到 cyclin B1/Cdk1 复合物的调节，cyclin B1 是该复合物的催化亚基. Cyclin B1 开始出现于 S 期末，在 G2 期逐渐增加，M 期起始时从胞质进入胞核[17]. Cyclin B1 与 Cdk1 结合后使后者激活，促发有丝分裂起始[20]. 在有丝分裂早中期末、中期初始，cyclin B1 开始降解，到晚期开始时绝大多数 cyclin B1 已经被降解[21]. Cyclin B1 降解导致 cyclin B1/Cdk1 复合物失活，细胞退出有丝分裂[22]. 实验结果显示，PAB 作用后 MCF-7 细胞的 cyclin B1 含量增加，这一点也提示 G2 和 M 期细胞比例有所增加. 通过 pHH3 荧光强度把细胞分成两群——M 期细胞和间期细胞，分别检测二者的 cyclin B1 含量，结果显示无论是阴性对照还是 PAB 作用后，M 期细胞的 cyclin B1 含量都要高于间期细胞. 同时，从高内涵分析获取的荧光图片

可见阴性对照孔有典型的 M 期中期细胞(形成赤道板和两极纺锤体)，较高浓度(≥2.5 μmol/L)的 PAB 作用后，M 期细胞染色体凝集却未见赤道板和二极纺锤体，呈现出早中期有丝分裂细胞的表现. 5、10 μmol/L PAB 可使微管染色变淡，定量结果显示细胞微管蛋白荧光强度减弱. 因为细胞打孔之后游离状态的微管蛋白会透出细胞膜，最后荧光染色所见的主要是聚合成微管的微管蛋白，所以微管蛋白荧光强度减弱提示 PAB 促进微管解聚这与其他文献微管蛋白聚合实验的结果是一致的[11, 18]. 由此推测，PAB 可能通过促进微管蛋白解聚干扰正常纺锤体形成，使染色体不能与纺锤体正确结合，激活有丝分裂检验点，导致 cyclin B1 等调节有丝分裂中、后期转换的蛋白质不能降解，引起有丝分裂阻滞[23].

PAB 作用后的 MCF-7 细胞出现“葡萄串样”的巨型细胞核. 高内涵法定量结果显示细胞核的平均大小和边缘不规则程度都有增加. 推测部分 MCF-7 细胞在被阻滞于 M 期之后没有保持阻滞状态，而是在未发生细胞分裂的情况下退出 M 期重新进入 G1 期，即发生了有丝分裂滑脱[24]. 有丝分裂滑脱的机制尚未阐明，有文献认为可能与药物干扰细胞的微管组装状态有关，也与 cyclin B 持续缓慢的降解有关[25-26]. 另外，流式细胞术 annexin Ⅴ-FITC 和 PI 双染显示 PAB 可导致 MCF-7 细胞凋亡，高内涵分析显示 PAB 可导致线粒体增生，而线粒体增生可见于细胞凋亡等情况[27]. 据文献报道，抗有丝分裂药物作用之后，细胞可能有多种表现——维持有丝分裂阻滞状态直至药物被移除，直接在有丝分裂阻滞时死亡，发生有丝分裂滑脱重新进入 G1 期[28]. 而细胞发生有丝分裂滑脱之后，可能继续细胞周期循环或者发生死亡[28]. PAB 导致的细胞凋亡是发生在 M 期还是发生在有丝分裂滑脱之后，尚需进一步研究.

高内涵分析是一种综合性的方法，具备荧光显微术、免疫印迹技术、流式细胞术的部分功能，既能提供细胞形态学信息，也能对特定荧光靶点进行定量和定位，还可以根据特定标准把细胞分成相应亚群进行单独分析. 高内涵分析主要是在微量培养板(96 孔、384 孔)上进行的，对细胞、试剂的需求量较少，而细胞染色之后的荧光激发、图片采集和分析过程高度自动化，可以减小工作量、减少实验人员主观判断失误对实验结果的影响(比如计算有丝分裂指数时). 高内涵分析有助于研究以有丝分裂为靶的药物作用机制.

综上所述，PAB 抑制 MCF-7 细胞增殖，该作用可能与其促进微管蛋白解聚、干扰二极纺锤体形成、阻滞有丝分裂有关，PAB 促进 MCF-7 细胞凋亡，该作用可能与其促进线粒体增生有关. 而 PAB 导致的有丝分裂阻滞与有丝分裂滑脱、凋亡之间的具体关系，以及除了凋亡之外细胞有没有其他死亡方式(比如有丝分裂灾变[29])尚需要进一步研究.

参 考 文 献

[1] Yang S P, Dong L, Wang Y, *et al*. Antifungal diterpenoids of Pseudolarix kaempferi, and their structure-activity relationship study. Bioorg Med Chem, 2003, **11**(21): 4577-4584

[2] Pan D J, Li Z L, Hu C Q, *et al*. The cytotoxic principles of Pseudolarix kaempferi: pseudolaric acid-A and -B and related derivatives1. Planta Med, 1990, **56**(4): 383-385

[3] Ma G, Chong L, Li X C, *et al*. Selective inhibition of human leukemia cell growth and induction of cell cycle arrest and apoptosis by pseudolaric acid B. J Cancer Res Clin Oncol, 2010, **136**(9): 1333-1340

[4] Wong V K W, Chiu P, Chung S S M, *et al*. Pseudolaric acid B, a novel microtubule-destabilizing agent that circumvents multidrug resistance phenotype and exhibits antitumor activity *in vivo*. Clin Cancer Res, 2005, **11**(16): 6002-6011

[5] Li K S, Gu X F, Li P, *et al*. Effect of pseudolaric acid B on gastric cancer cells: inhibition of proliferation and induction of apoptosis. World J Gastroenterol, 2005, **11**(48): 7555-7559

[6] Wu W Y, Guo H Z, Qu G Q, *et al*. Mechanisms of pseudolaric acid B-induced apoptosis in Bel-7402 cell lines. Am J Chinese Med, 2006, **34**(5): 887-899

[7] Ko J K S, Leung W C, Ho W K, *et al*. Herbal diterpenoids induce growth arrest and apoptosis in colon cancer cells with increased expression of the nonsteroidal anti-inflammatory drug-activated gene. Eur J Pharmacol, 2007, **559**(1): 1-13

[8] Yu J H, Wang H J, Li X R, *et al*. Protein tyrosine kinase, JNK, and ERK involvement in pseudolaric acid B-induced apoptosis of human breast cancer MCF-7 cells. Acta Pharmacol Sin, 2008, **29**(9): 1069-1076

[9] Gong X F, Wang M W, Tashiro S I, *et al*. Involvement of JNK-initiated p53 accumulation and phosphorylation of p53 in pseudolaric acid B induced cell death. Exp Mol Med, 2006, **38**(4): 428-434

[10] Gong X F, Wang M W, Tashiro S, *et al*. Pseudolaric acid B induces apoptosis through p53 and Bax/Bcl-2 pathways in human melanoma A375-S2 cells. Arch Pharm Res, 2005, **28**(1): 68-72

[11] Tong Y G, Zhang X W, Geng M Y, *et al*. Pseudolarix acid B, a new tubulin-binding agent, inhibits angiogenesis by interacting with a novel binding site on tubulin. Mol Pharmacol, 2006, **69**(4): 1226-1233

[12] Li M H, Miao Z H, Tan W F, *et al*. Pseudolaric acid B inhibits angiogenesis and reduces hypoxia-inducible factor 1α by promoting proteasome-mediated degradation. Clin Cancer Res, 2004, **10**(24): 8266−8274

[13] Giuliano K A, Debiasio R L, Dunlay R T, *et al*. High-content screening: A new approach to easing key bottlenecks in the drug discovery process. J Biomol Screen, 1997, **2**(4): 249−259

[14] Abraham V C, Taylor D L, Haskins J R. High content screening applied to large-scale cell biology. Trends Biotechnol, 2004, **22**(1): 15−22

[15] Skehan P, Storeng R, Scudiero D, *et al*. New colorimetric cytotoxicity assay for anticancer-drug screening. J Natl Cancer Inst, 1990, **82**(13): 1107−1112

[16] Gimarx K A, O'neil P, Hoffman P, *et al*. Data mining the NCI cancer cell line compound GI_{50} values: identifying quinone subtypes effective against melanoma and leukemia cell classes. J Chem Inf Comput Sci, 2003, **43**(5): 1652−1667

[17] Gasparri F, Cappella P, Galvani A. Multiparametric cell cycle analysis by automated microscopy. J Biomol Screen, 2006, **11**(6): 586−598

[18] Wong V K W, Chiu P, Chung S S M, *et al*. Pseudolaric acid B, a novel microtubule-destabilizing agent that circumvents multidrug resistance phenotype and exhibits antitumor activity *in vivo*. Clin Cancer Res, 2005, **11**(16): 6002−6011

[19] Shao R G, Cao C X, Shimizu T, *et al*. Abrogation of an S-phase checkpoint and potentiation of camptothecin cytotoxicity by 7-hydroxystaurosporine (UCN-O1) in human cancer cell lines, possibly influenced by p53 function. Cancer Res, 1997, **57**(18): 4029−4035

[20] Castedo M, Perfettini J L, Roumier T, *et al*. Cyclin-dependent kinase-1: linking apoptosis to cell cycle and mitotic catastrophe. Cell Death Differ, 2002, **9**(12): 1287−1293

[21] Clute P, Pines J. Temporal and spatial control of cyclin B1 destruction in metaphase. Nat Cell Biol, 1999, **1**(2): 82−87

[22] Weaver B A A, Cleveland D W. Decoding the links between mitosis, cancer, and chemotherapy: The mitotic checkpoint, adaptation, and cell death. Cancer Cell, 2005, **8**(1): 7−12

[23] Diaz-Martinez L A, Clarke D J. Chromosome cohesion and the spindle checkpoint. Cell Cycle, 2009, **8**(17): 2733−2740

[24] Riffell J L, Zimmerman C, Khong A, *et al*. Effects of chemical manipulation of mitotic arrest and slippage on cancer cell survival and proliferation. Cell Cycle, 2009, **8**(18): 3025−3038

[25] Andreassen P R, Margolis R L. Microtubule dependency of $p34^{cdc2}$ inactivation and mitotic exit in mammalian cells. J Cell Biol, 1994, **127**(3): 789−802

[26] Bíagosklonny M V. Mitotic arrest and cell fate: why and how mitotic inhibition of transcription drives mutually exclusive events. Cell Cycle, 2007, **6**(1): 70−74

[27] Camilleri-Broët S, Vanderwerff H, Caldwell E, *et al*. Distinct alterations in mitochondrial mass and function characterize different models of apoptosis. Exp Cell Res, 1998, **239**(2): 277−292

[28] Mcgrogan B T, Gilmartin B, Camey D N, *et al*. Taxanes, microtubules and chemoresistant breast cancer. Biochim Biophys Acta, 2008, **1785**(2): 96−132

[29] Mansilla S, Bataller M, Portugal J. Mitotic catastrophe as a consequence of chemotherapy. Anticancer Agents Med Chem, 2006, **6**(6): 589−602

Explore The Mechanism of Inhibitory Effects of Pseudolaric Acid B on MCF-7 Cells by High Content Analysis*

DUAN Shao-Wei, XU Bo, CHEN Yun-Li, LI Min, FU Hong-Zheng**, CUI Jing-Rong**

(*State Key Laboratory of Natural and Biomimetic Drugs, Peking University, Beijing* 100191, China)

Abstract Pseudolaric acid B (PAB), a major biologically active component of "TuJinPi" (the root bark of *Pseudolarix kaemferi* Gordon), exhibited cytotoxicity in many human tumor cell lines. High content analysis (HCA) is a fluorescence microscopy-based automated technology used for quantitative analysis of multiple targets in cells. HCA could yield rich information about the temporal-spatial dynamics of the fluorescence-labeled cell constituents. The mechanism of inhibitory effects of pseudolaric acid B on human breast cancer MCF-7 cells was explored by high content analysis and flow cytometry. As shown by sulforhodamine B assay, PAB inhibited the proliferation of MCF-7 cells in a dose-dependent and time-dependent manner, and the 50% inhibition concentration (IC_{50}) for 72 h was (1.80±0.33) μmol/L. Flow cytometry (propidium iodide staining) showed that, after treatment with PAB for 24 h, the proportion of MCF-7 cells at G2/M phase could increase to about 93%. Flow cytometry (annexin V-FITC and propidium iodide staining) showed that, PAB induced apoptosis of MCF-7 cells. High content analysis showed that: after treatment with PAB for 16 h, the mitotic index of MCF-7 could increase to about 40%, and cyclin B1 was upregulated; PAB caused dose-dependent disassembly of microtubules and inhibited the formation of mitotic bipolar spindles; PAB induced increase of mitochondrial mass; PAB induced grape-like giant nuclei indicating mitotic slippage in MCF-7 cells. These results suggest that PAB inhibits MCF-7 cell proliferation and induces apoptosis, these inhibitory effects may be related to disassembly of microtubules, spindle abnormalities, mitotic arrest and increase of mitochondrial mass.

Key words high content analysis, pseudolaric acid B, MCF-7 cells, microtubule, mitotic arrest, apoptosis

DOI: 10.3724/SP.J.1206.2010.00335

*This work was supported by a grant from The 11th Five Years Key Programs for Science and Technology Development of China, Chinese National Significant Project of New Drugs Creation (2009ZX09301-010).

**Corresponding author.

CUI Jing-Rong. Tel: 86-10-82802467, E-mail: jrcui@bjmu.edu.cn

FU Hong-Zheng. Tel: 86-10-82805212, E-mail: drhzfu@yahoo.com.cn

Received: June 25, 2010 Accepted: September 30, 2010